

11-17-TD  
134251**P1.5A THE USE OF A SATELLITE CLIMATOLOGICAL DATA SET TO INFER LARGE SCALE  
THREE DIMENSIONAL FLOW CHARACTERISTICS**

Jeffrey A. Lerner \*  
Global Hydrology and Climate Center  
University of Alabama in Huntsville  
Huntsville, Alabama

Gary J. Jedlovec  
Global Hydrology and Climate Center  
NASA/Marshall Space Flight Center  
Huntsville, Alabama

Robert J. Atkinson  
Global Hydrology and Climate Center  
Lockheed Martin  
Huntsville, Alabama

**1. INTRODUCTION**

Ever since the first satellite image loops from the 6.3  $\mu\text{m}$  water vapor channel on the METEOSAT-1 in 1978, there have been numerous efforts (many to a great degree of success) to relate the water vapor radiance patterns to familiar atmospheric dynamic quantities. The realization of these efforts is becoming evident with the merging of satellite derived winds into predictive models (Velden et al., 1997; Swadley and Goerss, 1989). Another parameter that has been quantified from satellite water vapor channel measurements is upper tropospheric relative humidity (UTH) (e.g., Soden and Bretherton, 1996; Schmetz and Turpeinen, 1988). These humidity measurements, in turn, can be used to quantify upper tropospheric water vapor and its transport to more accurately diagnose climate changes (Lerner et al., 1998; Schmetz et al. 1995a) and quantify radiative processes in the upper troposphere. Also apparent in water vapor imagery animations are regions of subsiding and ascending air flow. Indeed, a component of the translated motions we observe are due to vertical velocities. The few attempts at exploiting this information have been met with a fair degree of success. Picon and Desbois (1990) statistically related Meteosat monthly mean water vapor radiances to six standard pressure levels of the European Centre for Medium Range Weather Forecast (ECMWF) model vertical velocities and found correlation coefficients of about 0.50 or less. Synoptic scale vertical displacements were quantified by Stout et al. (1984) from GOES Visible Infrared Spin Scan Radiometer (VISSR) Atmospheric Sounder (VAS) brightness temperature ( $T_B$ ) measurements. They found vertical displacements on the order of  $1 \mu\text{b s}^{-1}$  in a case study over the Atlantic Ocean during summer.

It is hypothesized in the current study that in regions void of diabatic heating, vertical motions may be inferred along an isentropic surface which can be approximated by the pressure height estimated from satellite measurements and a nearby temperature profile.

This paper presents some preliminary results of viewing climatological satellite water vapor data in a different fashion. Specifically, we attempt to infer the three dimensional flow characteristics of the mid- to upper troposphere as portrayed by GOES VAS during a warm ENSO event (1987) and a subsequent cold period in 1988.

**2. METHODOLOGY**

To demonstrate how GOES winds may be used to infer the three-dimensional flow characteristics of the middle and upper troposphere, we first convey to the reader how water vapor imagery may be viewed as a nearly constant moisture layer that varies in height. Next, horizontal wind streamlines are displayed to locate regions where rising motion or subsidence might be expected. As a first attempt to validate our qualitative inferences, we display NCEP reanalysis (Kalnay et al., 1996) vertical velocity pressure level data. The satellite quantities estimated in this paper are derived from water vapor winds using GOES-7 VAS 6.7  $\mu\text{m}$  channel data during June, July, and August (JJA) of 1987 and 1988. This section briefly summarizes the algorithm used for calculating water vapor wind vectors and our approach to assigning wind vector heights.

**2.1 GOES Winds**

Winds were derived using the Marshall Automated Wind (MAW) algorithm (Atkinson, 1987; Jedlovec and Atkinson, 1998) which uses minimum-difference template matching for feature tracking. Three water vapor images (1100, 1200, and 1300 GMT) were used to determine a pair of wind vectors for each template of the image. The

\*Corresponding author address: Jeffrey A. Lerner, Global Hydrology and Climate Center, University of Alabama in Huntsville, 977 Explorer Blvd., Huntsville, Alabama 35806; e-mail <lerner@atmos.uah.edu>.

template is used to mathematically track the movement of a feature from image-to-image. For the current study, the MAW algorithm was applied using a  $25 \times 49$  template of  $16 \times 8$  km pixels. This produces a spatial resolution of about 400 km between adjacent wind vectors. Daily winds were produced for each day of June, July, and August of 1987 and 1988. The current quality control procedures include the elimination of vector pair discrepancies of  $15 \text{ ms}^{-1}$  in speed and 30 degrees in direction. Using these quality and control procedures, random errors in GOES VAS data are reduced to less than  $4 \text{ ms}^{-1}$  (Jedlovac and Atkinson 1996). After the vector pair discrepancy quality control step, visual analysis of the individual vectors is carried out to eliminate obvious vectors that are in error (usually occurring in areas of little or no structure in the water vapor field).

## 2.2 Wind Vector Heights

The simple height assignment approach for this study incorporates NCEP model reanalysis temperature profile information at 1200 UTC daily for locating the pressure at which the corresponding satellite  $T_B$  is equivalent to the model thermometric temperature. This level approximates the mean level where contribution to the measured  $T_B$  is usually greatest. However, the layer contributing to the satellite measured  $T_B$  varies in depth and height due to the water vapor profile, to a lesser extent the temperature profile, and also due to the satellite instrument view angle (Fischer et al., 1982). Different cloud types also contribute to the shape of the weighting function profile.

## 3. RESULTS

Because water vapor emissions of absorbed terrestrial radiation in the 6-7  $\mu\text{m}$  infrared absorption band are almost entirely due to water vapor in the middle and upper troposphere, the satellite signal becomes saturated at a nearly constant amount of absolute humidity in cloudless areas. Stout et al. (1984) determined that the amount of precipitable water (PW) above the water vapor "upper boundary" to vary between 0.5-1.5 mm with GOES-VAS when correlated with a nearby radiosonde profile. Schmetz et al. (1995b), found Meteosat-4 measurements to be sensitive to the upper 3 mm of PW. In our applications, a radiative transfer model was used to simulate the GOES VAS weighting function profile and channel

brightness temperature. Using the Air Force Geophysical Laboratory (AFGL) standard tropical profile, we found GOES-VAS sensitive to about the top 2 mm of PW. This was determined by vertically integrating the specific humidity and multiplying each atmospheric layer by the corresponding normalized weight determined from the instrument spectral response or

$$PW = \sum_{i=0}^{sfc} \left[ \bar{q}_i \frac{dp_i}{g} \times W_i \right]$$

(Figure 1). This amount of moisture varies with satellite water vapor channel spectral characteristics (e.g., channel spectral bandwidth and center wavelength).

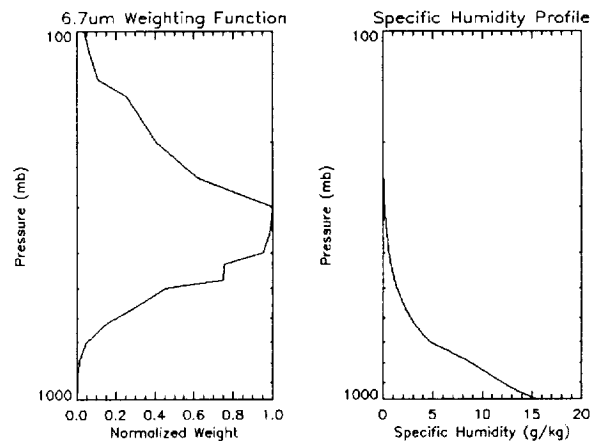


Figure 1: Simulated GOES - VAS 6.7  $\mu\text{m}$  channel weighting function profile and specific humidity (g/kg) profile using the AFGL standard tropical atmosphere.

The hypothesis in the introduction stated that the derived water vapor wind heights from GOES approximate an isentropic surface such that vertical motions may be inferred from cross-isobaric flow. Typically we view isentropes in two dimensional vertical cross sections at synoptic scales to identify air masses, fronts, and regions of rising and sinking motion near mid-latitude baroclinic zones. For this study, we extend our view of an isentropic layer over the GOES viewing area. Indeed, potential temperature will not be constant in the water vapor layer owing to errors that arise in the height assignments (due to assumptions made and model inaccuracies in temperature profile) and also due to the presence of diabatic processes such as radiative heating/cooling and evaporation/condensation. By time averaging the data, we reduce the diabatic effects that occur on small time and space scales. Our results indicate that the potential temperature

( $\theta$ ) does vary by as much as 20 K from the mid latitudes to the tropics. However, large regions are characterized by nearly constant  $\theta$  in which our hypothesis is valid. For simplicity, at this time we assume that the flow generally adheres to the layer defined by the water vapor wind heights so that a first order approximation of the vertical motion characteristics may be made.

The flow pattern derived from taking the mean of daily winds during JJA of 1987 and 1988 is displayed in figures 2a and 2b. The streamlines (solid lines) are overlaid on the assigned pressure height (dashed lines). It is readily apparent that in 1988 southwestward flow into the dry subtropics is dominant south of 15° N across the GOES-7 viewing domain. The winds shift southwestward south of a ridge axis near 5-10° S towards the southern hemisphere subtropical jet stream. In 1987, the flow pattern is in stark contrast to the cold La Nina event of 1988. For example, in the tropical Atlantic, more "typical" southeasterlies are observed to form a ridge axis near 10° N.

The contours of pressure height are also shown to highlight the large scale subsidence and rising motion areas that might be expected. Assuming that diabatic processes are small in a mean sense, the flow pattern along the derived water vapor heights should approximate flow on an adiabatic surface. South of 5° N, flow tends to descend which is consistent with zonally averaged estimates of vertical velocities from the NCEP reanalysis model pressure level data (Figure 3). However, even at large time and space scales, the adiabatic assumption is not as strong near the Inter Tropical Convergence Zone (ITCZ) and mid-latitude baroclinic zones. This is why we don't see cross-isobaric flow in regions of tropical convection. Rather, upper-level wind divergence patterns (not shown) are associated with regions of deep convection where rising motion and strong diabatic heating (due to condensation in precipitating convective systems) are present.

In Figure 2a, divergent centers can be observed along the ITCZ over Central America. In 1988, these centers aren't apparent, but the strong cross-isobaric flow in the tropical east Pacific is still present. The pressure gradient along the streamlines in this subsidence region is approximately 5 mb/100 km. With a typical wind speed of 10 m/s, a rough estimate of the subsidence is 0.5  $\mu\text{b/s}$  ( $\sim 1$  cm/s) which is consistent with typical tropical subsidence rates given by Holton (1979).

Another interesting feature from this figure worth noting is the detection of northwesterlies over the eastern half of the United States. The implications of this type of pattern are drier conditions which is consistent with the severe drought endured during the summer of 1988.

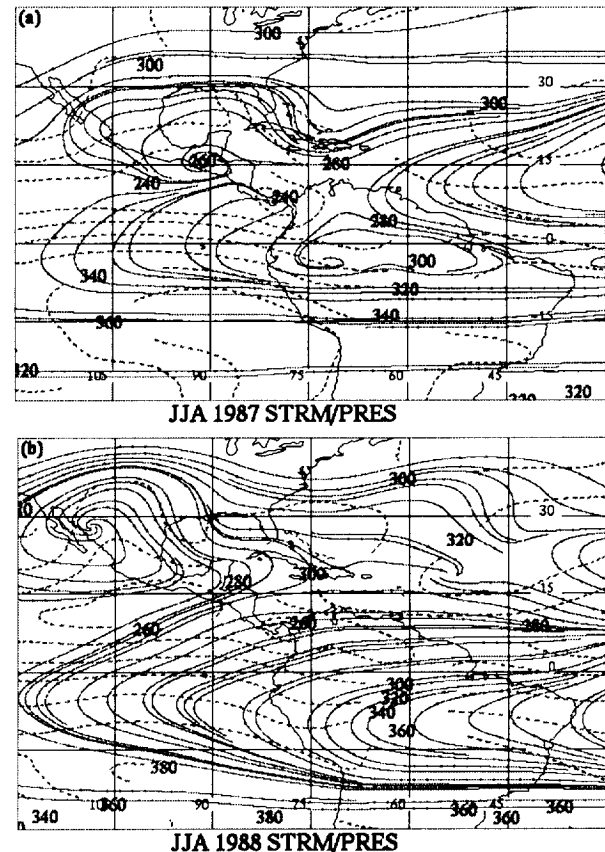


Figure 2: Summer averaged pressure height of the water vapor wind vectors (dashed contours) overlaid on streamlines of the summer mean flow for 1987 (a) and 1988 (b).

Typically, dark bands in the water vapor imagery are associated with dry subsidence zones (e.g. behind cold fronts and in subtropical highs). The height assignments in these dark regions are lower in the atmosphere (higher pressure) owing to the drier upper troposphere (water vapor emissions from lower levels). In Figure 3, the zonal mean NCEP Reanalysis vertical velocities (VVEL) (cm/s) at 400 mb are plotted below the zonal mean pressure height (mb) of the GOES water vapor winds. The zonal mean values are averaged over 30°-120° W. The phases of these two plots show good agreement. The strongest positive vertical velocities near 10° N are associated with the highest height assignment levels corresponding to the coldest brightness temperatures observed in the ITCZ. The strongest subsidence according to

the model data is near 20° S which corresponds to the lowest height assignment level in the GOES wind vectors. At this latitude in the southern hemisphere winter, the subtropical high is well established across the GOES viewing domain. The interannual variations in the zonal means of pressure height are subtle but show that in 1988 the upper troposphere was generally drier (lower height assignments) across all latitudes. The interannual variation in VVEL indicates good agreement at most latitudes with the exception of stronger subsidence extending further south in the southern hemisphere during JJA 1988.

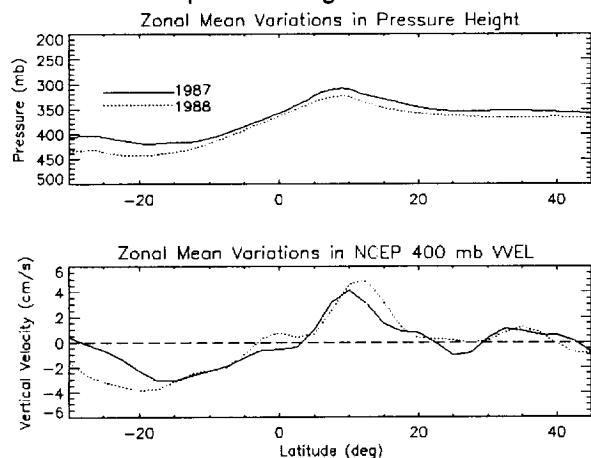


Figure 3: Zonal mean pressure height (mb) of the water vapor winds for 1987 (solid) and 1988 (dotted). Bottom plot displays zonal mean vertical velocities (cm/s) at 400 mb estimated by the NCEP reanalysis model.

#### 4. SUMMARY

The preliminary results presented in this conference paper have shown promise in the final goal of being able to quantify vertical motions from water vapor channel satellite measurements. It was shown that cross-isobaric flow in the GOES measurements is consistent with regions of subsidence portrayed by the NCEP reanalysis model. While our current methodology and results only is a cursory glance at the potential of deriving vertical velocities from long term satellite data, it does not test the original hypothesis that the water vapor layer derived using water vapor wind heights behaves like an isentropic surface. The relative magnitude of diabatic effects needs to be estimated to delineate which regions vertical motions may be quantified with greater confidence. To produce quantitative results from the satellite measurements, a kinematic or adiabatic model needs to be developed that takes advantage of the spatial and temporal changes in the water vapor

winds, temperature, and heights. More recent results from these ongoing efforts will be presented on the poster at the conference.

#### 5. REFERENCES

- Atkinson, R. J., 1987: Automated mesoscale winds determined from satellite imagery. *Final Report on NAS8-34596*, General Electric Company, Huntsville, AL, 50 pp.
- Fischer, N., N. Eigenwillig, and H. Muller, 1982: Information content of METEOSAT and Nimbus/THIR water vapor channel data: Altitude association of observed phenomena. *J. Appl. Meteor.*, **20**, 1344-1352.
- Holton, J. R., 1979: *An Introduction to Dynamic Meteorology*. Academic Press, San Diego, 512 pp.
- Jedlovec, G. J., and R. J. Atkinson, 1998: The Marshall Automated Wind algorithm for geostationary satellite wind applications. *Proc. of the Ninth Conf. on Sat. Meteor. and Oceanog.*, AMS, Paris, France, P3.6B.
- Jedlovec, G. J., and R. J. Atkinson, 1996: Quality and control of water vapor winds. *Proc. of the Eighth Conf. on Sat. Meteor. and Oceanog.*, AMS, Boston, 5-9.
- Kalnay, E., M. Kanamitsu, R. Kistler, W. Collins, D. Deaven, L. Gandin, M. Iredell, S. Saha, G. White, J. Woollen, Y. Zhu, M. Chelliah, W. Ebisuzaki, W. Higgins, J. Janowiak, K. C. Mo, C. Ropelewski, J. Wang, A. Leetmaa, R. Reynolds, R. Jenne, and D. Joseph, 1996: The NCEP/NCAR 40-year reanalysis project. *Bull. Amer. Meteor. Soc.*, **77**, 437-471.
- Lerner, J. A., G. J. Jedlovec, and R. J. Atkinson, 1998: Observed changes in upper-tropospheric water vapor transport from satellite measurements during the summers of 1987 and 1988. *Proc. of the Ninth Symp. on Global Change Studies*, AMS, Long Beach, Calif., 23-26.
- Picon, L., and M. Desbois, 1990: Relation between METEOSAT water vapor radiance fields and large scale tropical circulation features. *J. Climate*, **3**, 865-876.
- Schmetz, J., W. P. Menzel, C. Velden, X. Wu, L. van de Berg, S. Nieman, C. Hayden, K. Holmlund, and C. Geijo, 1995a: Monthly mean large scale analysis of upper troposphere humidity and wind field divergence derived from three geostationary satellites. *Bull. Amer. Meteor. Soc.*, **76**, 1578-1584.
- Schmetz, J., C. Geijo, W. P. Menzel, K. Strabala, L. van de Berg, K. Holmlund, and S. Tjemkes, 1995b: Satellite observations of upper troposphere relative humidity, clouds, and wind field divergence. *Beitr. Phys. Atmosph.*, **68**, 345-357.
- Soden, B. J., and F. P. Bretherton, 1996: Interpretation of TOVS water vapor radiances in terms of layer-average relative humidities: Method and climatology for the upper, middle, and lower troposphere. *J. Geophys. Res.*, **101**, 9333-9343.
- Stout, J., J. Steranka, and R. A. Petersen, 1984: Vertical displacements of the mid-tropospheric water vapor boundary in the tropics derived from the VISSR Atmospheric sounder (VAS) 6.7  $\mu$ m channel. *Proc. AMS Conf on Sat. Remote Sensing and Appl.*, Clearwater Beach, FL 86-89.
- Swadley, S. D., and J. S. Goerss, 1989: Assimilation of automated winds derived from GOES multispectral imagery. *Preprints Fourth Conf. on Sat. Meteor. and Oceanog.*, AMS, San Diego, Calif., 242-245.
- Schmetz, J., and O. M. Truinen, 1988: Estimation of the upper tropospheric relative humidity field from METEOSAT water vapor image data. *J. Appl. Meteor.*, **27**, 889-899.